U.S. DEPARTMENT OF COMMERCE
NATIONAL OCEANIC AND ATMOSPHERIC ADMINISTRATION
NATIONAL WEATHER SERVICE
SYSTEMS DEVELOPMENT OFFICE
TECHNIQUES DEVELOPMENT LABORATORY

TDL Office Note 75-8

SIMPLE PROPERTIES OF CHAPEAU FUNCTIONS AND THEIR APPLICATION TO THE SOLUTION OF THE ADVECTION EQUATION

Paul E. Long, Jr. and Farnese J. Hicks

October 1975

Simple Properties of Chapeau Functions and Their Application to the Solution of the Advection Equation

by

Paul E. Long, Jr. and Farnese J. Hicks

ABSTRACT. This note is devoted to the derivation and simple application of chapeau functions. The concept of the Galerkin method for the solution of partial differential equations is introduced, a special case of which is the chapeau function technique. Chapeau functions are used for approximating solutions of linear and non-linear advection equations after certain basic relationships are derived.

1. Introduction

Our decision to use an implicit chapeau function technique in the TDL 3-dimensional boundary layer model [1] was based upon the need to integrate the predictive boundary layer equations efficiently and with reasonable accuracy. The use of an implicit finite difference scheme for integrating the vertical turbulent transfer equations was largely forced upon us; explicit schemes which remain stable with large time steps all seem to suffer badly from consistency problems [2]. The need for an implicit scheme in the horizontal portions of the predictive equations is much less crucial than for the vertical, provided we retain our 80 km horizontal mesh spacing. However, since it is very probable that we will begin experimenting with refined meshes and 2-dimensional telescoping grids in the near-future, we decided in favor of the extra numerical stability of an implicit scheme.

Some initial calculations with one of the simplest and best-known of the implicit schemes, the Crank-Nicolson advection scheme, along with other implicit techniques derived from conventional explicit schemes were not encouraging. Although more stable, the implicit schemes had worse phase errors and computational damping than many standard explicit schemes.

The Crank-Nicolson scheme can be improved by replacing the spatial difference derivative, correct to order $\mathcal{O}(\Delta x^2)$[1], by a spatial derivative correct to order $\mathcal{O}(\Delta x^4)$:

$$\frac{Q_j^{n+1} - Q_j^n}{\Delta t} + \frac{U}{2\Delta x}\left(\delta\, Q_j^{n+1} + \delta\, Q_j^n\right) = 0; \quad \mathcal{O}(\Delta x^2) \qquad 1.1$$

---

1 See Appendix I for definition of symbols.

$$\frac{Q_j^{n+1} - Q_j^n}{\Delta t} + \frac{U}{2\Delta x}(D_x Q_j^{n+1} + D_x Q_j^n) = 0; \quad \mathcal{O}(\Delta x^4) \qquad 1.2$$

where $\delta Q_j = \left(\frac{Q_{j+1} - Q_{j-1}}{2} \right)$

Here n and j are the indices of the time and space respectively, and D_x is the fourth-order central difference operator with the following effect upon the operand, Q_j:

$$D_x Q_j = 2/3\ (Q_{j+1} - Q_{j-1}) - 1/12\ (Q_{j+2} - Q_{j-2}) \qquad 1.3$$

The second-order scheme forms a tri-diagonal matrix system that is very easy to solve [3]; the fourth-order scheme is less easily dispatched.

As an alternative, Dr. James Bradley of Drexel University suggested a Galerkin technique using chapeau basis function. The Galerkin method is frequently employed in engineering problems to find approximate analytical solutions of differential equations. (It is interesting to note that Galerkin, a Russian Engineer, published his first paper while in a Tsarist political prison [4].)

2. The Galerkin Method and Chapeau Functions

If one approximates the solution to a differential equation, for example Laplace's equation,

$$\left(\frac{\partial^2}{\partial x^2} + \frac{\partial^2}{\partial y^2} \right) Q(x,y) = 0 \qquad 2.1$$

by an expansion (repeated subscripts will be summed) of suitable basis functions $e_i(x,y)$,

$$Q(x,y) \triangleq \sum_i \alpha_i e_i(x,y) \equiv \alpha_i e_i(x,y) \qquad 2.2$$

then the differential equation will be approximated* with a residual R,

$$\alpha_i \left(\frac{\partial^2 e_i}{\partial x^2} + \frac{\partial^2 e_i}{\partial y^2} \right) = R(x,y) \qquad 2.3$$

If one then demands that the residual R(x,y) be orthogonal** to each of the basis functions,

$$\int dx\,dy\, R(x,y) e_j(x,y) = 0 \qquad 2.4$$

---

* We use $\triangleq$ to denote approximate equality

** Two functions f(x), g(x) are orthogonal if $\int dx fg = 0$.

then the resulting solution is a solution obtained by Galerkin's method. As another example, let us take the simple advection equation

$$\frac{\partial Q}{\partial t} + U\frac{\partial Q}{\partial x} = 0; \quad U = \text{constant} \qquad 2.5$$

and approximate the solution by basis functions $e_i(x)$ and time-varying coefficients $\alpha_i(t)$

$$Q(x,t) = \alpha_i(t)\, e_i(x) \qquad 2.6$$

The Galerkin method demands,

$$\frac{d\alpha_i(t)}{dt} \int dx\, e_i(x)e_j(x) + \alpha_i(t)\; U \int dx\, e_i'(x)e_j(x)$$

$$\equiv M_{ji}\frac{d\alpha_i(t)}{dt} + UN_{ji}\alpha_i(t) = 0 \qquad 2.7$$

where $M_{ji} = M_{ij} \equiv \int dx\, e_i(x)\, e_j(x)$

and $N_{ji} = N_{ij} = \int dx\, e_i'(x)\, e_j(x)$

If, as is often the case, the trial functions are orthogonal, then

$$M_{ij} = m_i\delta_{ij} \quad \text{and} \quad \frac{d\alpha_i(t)}{dt} + \frac{N_{ji}\alpha_i(t)}{m_i} = 0. \qquad 2.8$$

Suitable basis functions might include trigonometric functions, Legendre polynomials, etc.

We shall choose instead piecewise continuous "chapeau" functions, so-called because each function looks like a hat [Fig. 1]. The figure shows linear chapeau functions defined by the relations

$$e_j(x) = \frac{x - x_{j-1}}{x_j - x_{j-1}} \qquad x_{j-1} \le x \le x_j$$

$$e_j(x) = \frac{x_{j+1} - x}{x_{j+1} - x_j} \qquad x_j \le x \le x_{j+1} \qquad 2.9$$

$$e_j(x) = 0 \qquad \text{otherwise}$$

Although we shall consider only linear chapeau functions in this note, other basis function which vanish outside the interval $[x_{j-1}, x_{j+1}]$ are possible, also.

To apply the linear functions to the simple advection problem we need only to compute M_{ij} and N_{ij}. Unfortunately, chapeau functions are not orthogonal functions; the scalar products $\int dx e_j(x)e_{j\pm 1}(x)$ do not vanish (no summation over j).

We must compute the scalar products indicated by the following figure.

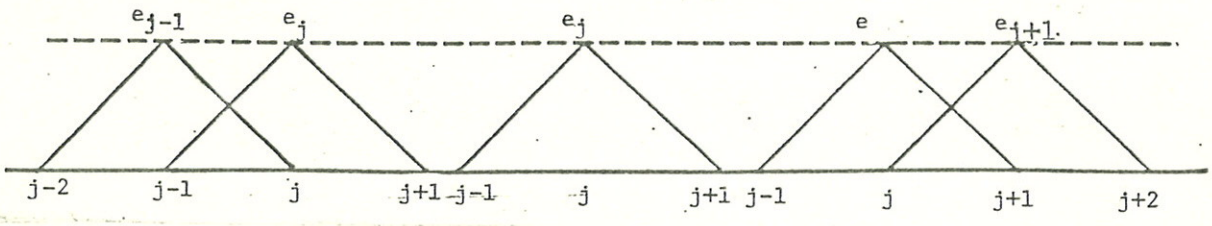

If the spacing between the node points is constant and set equal to Δx, then

$$\int dx\ e_j\ e_{j+1} = \int dx\ e_j e_{j-1} = \frac{\Delta x}{6} \qquad 2.10$$

and

$$\int dx\ e_j e_j dx = \int dx\ e_j^2 = \frac{2\Delta x}{3} \qquad 2.11$$

Thus we have

$$M_{ij} = \left(\frac{1}{6}\delta_{i,j+1} + \frac{2}{3}\delta_{ij} + \frac{1}{6}\delta_{i,j-1} \right) \qquad 2.12$$

Similarly,

$$\begin{aligned} \int dx\ e'_{j-1}\ e_j &= -\frac{1}{2} \\ \int dx\ e'_j e_j &= 0 \\ \int dx\ e'_{j+1}\ e_j &= \frac{1}{2} \end{aligned} \qquad 2.13$$

(no summation in the above relations). When we use these results, equation 2.5 reduces to

$$\frac{1}{6}\frac{d}{dt}\ (\alpha_{j-1} + 4\ \alpha_j + \alpha_{j+1}) + \frac{U}{2\Delta x}\ (\alpha_{j+1} - \alpha_{j-1}) = 0, \qquad 2.14$$

a difference-differential equation.

There are many ways of handling the equation as a difference equation, for example,

$$\begin{aligned} &\frac{d\alpha}{dt} \doteq \frac{\alpha^{n+1} - \alpha^n}{\Delta t}, \\ &\frac{U}{2\Delta x}\ (\alpha_{j+1} - \alpha_{j-1}) \doteq \frac{U}{2\Delta x}\left[\mu(\alpha^{n+1}_{j+1} - \alpha^{n+1}_{j-1}) + (1-\mu)\ (\alpha^n_{j+1} - \alpha^n_{j-1}) \right] \\ &\text{for } 0 \le \mu \le 1 \end{aligned} \qquad 2.15$$

where $\alpha^n_j = \alpha\ (x_j, t_n) = \alpha(j\Delta x, n\Delta t)$.

If the values of $Q(x_j, t = 0)$ are defined only at the mesh points x_j and the initial chapeau function solution collocates with the initial conditions, then the chapeau function equation reduces to the finite difference equation,

$$\frac{1}{6}\left[(Q_{j-1}^{n+1} - Q_{j-1}^{n}) + 4\ (Q_{j}^{n+1} - Q_{j}^{n}) + (Q_{j+1}^{n+1} - Q_{j+1}^{n})\right]$$
$$+\frac{R}{2}\left[\mu\ (Q_{j+1}^{n+1}) - Q_{j-1}^{n+1} + (1 - \mu)\ (Q_{j+1}^{n} - Q_{j-1}^{n})\right] = 0,$$

where $R = \dfrac{U\Delta t}{\Delta x}$

3. Properties of the chapeau function equation

To examine the stability of (2.16), we substitute $g^n \exp(i\lambda j\Delta x)$ into (2.16). After simplification the result is

$$g = \frac{1 + 1/2\ \cos\ \lambda\Delta x - 3iR/2\ (1 - \mu)\ \sin\ \lambda\Delta x}{1 + 1/2\ \cos\ \lambda\Delta x + 3iR\mu/2\ \ \sin\ \lambda\Delta x} \qquad 3.1$$

Here g stands for the amplification factor, λ the wavenumber ($\lambda = 2\pi/\text{wavelength} = 2\pi/L$), $i = \sqrt{-1}$ and R the Courant number.

The special case $\mu = 1/2$ is of particular interest; g may then be written as

$$g = \frac{1 + 1/2\ \cos(\lambda\Delta x) - 3iR/4\ \sin(\lambda\Delta x)}{1 + 1/2\ \cos(\lambda\Delta x) + 3iR/4\ \sin(\lambda\Delta x)} \qquad 3.2$$

The crucial factor with respect to computational stability is the magnitude of the complex quantity g. Since the numerator and the denominator are complex conjugates of each other, $g = 1$ for all Δt, Δx, and λ. This means the scheme is neutrally stable; there is neither amplification nor damping. Choosing $\mu < 1/2$ can lead to computationally unstable schemes (solutions amplifing). Setting $\mu > 1/2$ always gives stable schemes with heavy damping.

Since the numerator and denominator of (3.2) are of the form (a - bi) and (a + bi) respectively, g may be written as

$$g = e^{-2i\phi}$$

where ϕ is the real angle

$$\phi = \arctan\left[\frac{3/4\ R\ \sin(\lambda\Delta x)}{(1 + 1/2\ \cos\ (\lambda\Delta x))}\right]$$

The phase speed, c, of (3.2) can be computed from

$$C = \frac{\Theta}{\lambda\Delta t} \quad ; \quad g = |g|\ e^{i\Theta}$$

Curves of phase speeds of the chapeau function scheme and several other standard schemes are shown in Fig. 2. It is not difficult to see why the chapeau functions yield such accurate phase speeds in the linear case for relatively small time steps. If one takes

$$\frac{1}{6}\frac{d}{dt}\left(Q_{j-1} + 4Q_j + Q_{j+1}\right) + \frac{U}{2\Delta x}\left(Q_{j+1} - Q_{j-1}\right) = 0 \qquad 3.4$$

and performs a Taylor series expansion about $x = x_j$, then the result is

$$\frac{\partial Q}{\partial t} + U\frac{\partial Q}{\partial x} + \left(\frac{1}{120} - \frac{1}{72}\right) U\Delta x^4 \frac{\partial^5 Q}{\partial x^5} \doteq 0.$$

This means the scheme is accurate to order $\mathcal{O}(\Delta x^4)$. Although the stability is unlimited, increasingly larger time steps produce decreasingly accurate solutions.

4. The General Advection Equation

Let us now study the more general equation,

$$\frac{\partial Q}{\partial t} + u(x,t)\frac{\partial Q}{\partial x} = g(x,t) \qquad 4.1$$

As before, we set

$$Q(x,t) = \alpha_i(t)\, e_i(x) \qquad 4.2$$

and in addition,

$$u(x,t) = \beta_j(t)\, e_j(x). \qquad 4.3$$

The Galerkin method yields

$$\int dx\, e_k \left[\dot{\alpha}_i e_i + \alpha_i \beta_j e_i' e_j\right] - \frac{\Delta x}{6}\left(g_{j+1} + 4g_j + g_{j+1}\right) = 0. \qquad 4.4$$

We must now evaluate

$$\int dx\, e_k(x)\, e_i'(x)\, e_j(x).$$

Only nine terms must be considered. Using the notation $\int dx\, e_k\, e_i'\, e_j \equiv (k,i,j)$, we have,

$$\begin{aligned}
&1.\ (k,\ k,\ k) = 0 && 6.\ (k,\ k+1,\ k-1) = 0\\
&2.\ (k,\ k-1,\ k) = -1/3 && 7.\ (k,\ k+1,\ k+1) = 1/6\\
&3.\ (k,\ k+1,\ k) = 1/3 && 8.\ (k,\ k-1,\ k-1) = -1/6\\
&4.\ (k,\ k,\ k-1) = 1/6 && 9.\ (k,\ k-1,\ k+1) = 0\\
&5.\ (k,\ k,\ k+1) = -1/6
\end{aligned} \qquad 4.5$$

The general scheme then reduces to

$$\frac{d}{dt}\ (\alpha_{k-1} + 4\alpha_k + \alpha_{k+1}) + \frac{1}{\Delta x}[(2\beta_k + \beta_{k+1})\ \alpha_{k+1} - (\beta_{k+1} - \beta_{k-1})\alpha_k$$

$$- (2\beta_k + \beta_{k-1})\alpha_{k-1}] = g_{k-1} + 4g_k + g_{k+1} \qquad 4.6$$

5. Unequally Spaced Mesh Points

One of the features of the chapeau function scheme is the ease by which it can be extended to unequally spaced grid points. Using the irregularly spaced array

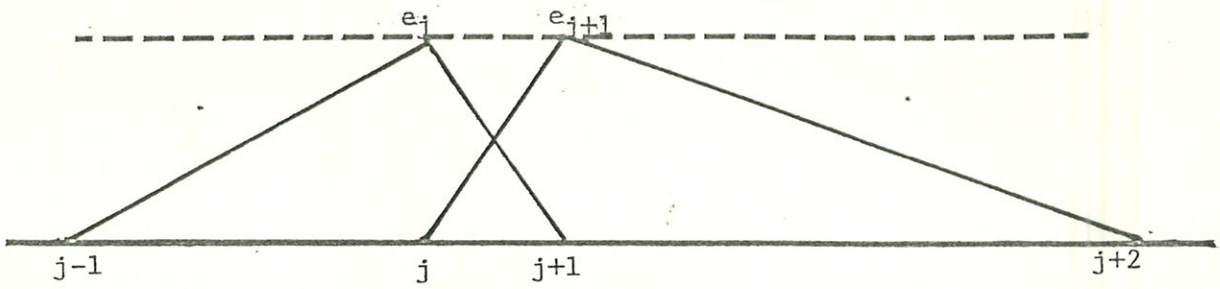

and the notation $h_j = x_{j+1} - x_j$, the new inner product (perhaps "tri-orthogonality" relation would be an appropriate term) becomes,

$$\int dx e_i(x)\ e_j(x) = \frac{1}{6}\ [h_{j-1}\delta_{i,j-1} + 2\ (h_j + h_{j-1})\ \delta_{i,j} + h_j\ \delta_{i,j+1}]\ . \qquad 5.1$$

It can be shown that the advective terms for both the simple linear and general case remain completely unaffected by the variable grid spacing. For the simple linear case,

$$\frac{h_{j-1}}{6}\ \dot{Q}_{j-1} + \frac{(h_j + h_{j-1})}{3}\ \dot{Q}_j + \frac{h_{j+1}}{6}\ \dot{Q}_{j+1}$$

$$+ \frac{U}{2}\ (Q_{j+1} - Q_{j-1}) = 0. \qquad 5.2$$

Variable grids are not without their problems. If a grid is divided into a fine-mesh and coarse-mesh region there will be reflections at the interface whenever a wave passes from one region to the other. We will show an example of this difficulty later.

6. Solution of the Implict Schemes

Both the simple linear case, (3.4) and the general case, (4.6), give systems of equations in which the value of Q_j^{n+1} is implicitly related to Q_{j+1}^{n+1} and Q_{j-1}^{n+1}. The system of unknowns becomes "tri-diagonal" when expressed in matrix form. We must solve the system

$$A_j Q_{j-1}^{n+1} + B_j Q_j^{n+1} + C_j Q_{j+1}^{n+1} = D_j \qquad 6.1$$

in which

$$\begin{aligned} A_j &= 1 - \Delta t/2\ (2U_j + U_{j-1}) \\ B_j &= 4 - \Delta t/2\ (U_{j+1} - U_{j-1}) \\ C_j &= 1 + \Delta t/2\ (2U_j + U_{j+1}) \\ D_j &= (Q_{j-1}^n + 4Q_j^n + Q_{j+1}^n) \\ &\quad - \Delta t/2\ (2U_j + U_{j+1})\ Q_{j+1}^n + \Delta t/2\ (U_{j+1} - U_{j-1})\ Q_j^n \\ &\quad + \Delta t/2\ (2U_j + U_{j-1})\ Q_{j-1}^n + \Delta t(g_{j-1} + 4g_j + g_{j+1}) \end{aligned} \qquad 6.2$$

The Thomas algorithim is used to solve the system. The solution is computed from the recursion relations

$$Q_{j+1}^{n+1} = \alpha_j Q_j^{n+1} + \beta_j \qquad E_j = B_{j+1} + \alpha_{j+1} C_{j+1}$$

$$\begin{aligned} \alpha_j &= -A_{j+1}/E_j \\ \beta_j &= (D_{j+1} - \beta_{j+1} C_{j+1})/E_j \end{aligned} \qquad 6.3$$

The first recursion relation is solved in the forward direction; the relations for α_j and β_j are computed backward. The starter relations for α_j and β_j are calculated from the boundary condition at gridpoint N:

$$\begin{aligned} \alpha_{N-1} &= \frac{-A_{N-1}}{B_{N-1}} \\ \beta_{N-1} &= \frac{D_N - C_{N-1} Q_N^{n+1}}{B_{N-1}} \end{aligned} \qquad 6.4$$

If Q_N^{n+1} is not given a priori but depends upon interior values (for example, $Q_N^{n+1} = Q_{N-1}^{n+1}$) the algorithm is changed only slightly.

7. Numerical Examples

A series of 1-dimensional examples is given in [3] along with a fairly lengthy discussion. We will give only the highlights.

In each case, linear and non-linear, the initial state is a Gaussian with a 1/e half-width of two grid intervals centered at $x = 10\Delta x$. The Gaussians ideally should advect at one grid interval per unit time for thirty time units.

Figures 3 and 4 compare the solutions of the chapeau and second-order Crank-Nicolson schemes for increasing Courant numbers ($R = U\Delta t/\Delta x$). Although for large Courant numbers ($R > 2.0$), the two schemes give nearly the same results, the superiority of the chapeau function scheme for smaller Courant numbers is evident. The reduction in the amplitudes comes about by the same mechanism as the creation of the wakes behind the Gaussian: the lagging phase velocity. There is no damping. Figure 5 shows that the solution for the non-linear case is distinguished from the linear case largely by the absence of the wake. This may be caused by the small local Courant numbers except near the center of the Gaussian.

The solution for the 2-dimensional linear case is discussed in the next section. We use Marchuk's concept of "splitting" to solve the 2-dimensional problem [5]. The idea is to solve the x and y direction

$$
\begin{aligned}
T_x \quad & \frac{(Q^{n+1/2} - Q^n)}{\Delta t} + \frac{L_x}{2}\,(Q^{n+1/2} + Q^n) = 0 \\
T_y \quad & \frac{(Q^{n+1} - Q^{n+1/2})}{\Delta t} + \frac{L_y}{2}\,(Q^{n+1} + Q^{n+1/2}) = 0 \qquad (7.1) \\
T_x \quad & Q_{i,j} = 1/6\,(Q_{i+1,j} + 4Q_{i,j} + Q_{i-1,j}) \\
L_x \quad & Q^n_{i,j} = U/2\Delta x\,(Q^n_{i+1,j} - Q^n_{i-1,j}).
\end{aligned}
$$

Here, T is the spatial averaging operator. L is the spatial differencing operator.

8. Boundary Conditions and "Ghosts"

When we used cubic splines [3], pseudo spectral techniques and chapeau functions for the solution of the linear advection equation on a limited area grid with fixed boundaries, we observed a remarkable phenomenon. When an object passed out from the forecast domain, a small amount of noise was generated at the outflow boundary. This noise quickly propagated upstream and collected at the fixed inflow boundary. The amassing of noise at the inflow region is caused by noise which moves rapidly against the flow but can move downstream only at about the same rate as the fluid. In each case, the noise regenerated either a fairly faithful reproduction (a "ghost") of the original Gaussian or gave its mirror (negative) image. With the cubic splines applied to a 2-dimensional limited area grid, the "ghost" was an

excellent recreation of the original Gaussian. The same procedure, applied to a 1-dimensional grid, gave a mirror image "ghost" (Fig. 6). Of course, we wish to exorcise such apparitions. This may be carried out fairly well by using the explicit upstream scheme,

$$\frac{Q_N^{n+1} - Q_N^n}{\Delta t} + UD\_\, Q_N^n = 0 \qquad 8.1$$

where D_ is a difference operator with the following effect on the operand,

$$D\_\, Q_j = \frac{Q_j - Q_{j-1}}{\Delta x} \qquad 8.2$$

solving for Q_N^{n+1},

$$Q_N^{n+1} = (1 + U\Delta t D\_)\, Q_N^n \,. \qquad 8.3$$

However, for large enough time steps the boundaries generate amplifying waves. We found the implicit-upstream scheme,

$$\frac{Q_N^{n+1} - Q_N^n}{\Delta t} + UD\_\, Q_N^{n+1} = 0 \qquad 8.4$$

completely stable. It reduced the noise substantially.* Since we must know Q_{N-1}^{n+1} to compute Q_N^{n+1}, the implicit upstream scheme must be incorporated into the tri-diagonal solution of the chapeau function technique. An example of its utility is shown in Fig. 7. We ran a 2-dimensional example in which a Gaussian was advected back and forth along the diagonal of a 25 x 25 square grid. The initial field Q (Fig. 7) is the 2-dimensional Gaussian with a half-width of 2 grid units, centered at point (10,10) with $\Delta x = \Delta y = 1$, and $\Delta t = 0.1$. The Gaussian's maximum value is 1. Advection velocities U and V are initially 1. Inflow boundary conditions were specified by the exact solution; outflow boundary values were computed using the implicit upstream (or downstream, for U<0) scheme. Whenever the center of the exact solution reached the corners (25,25) and (1,1) of the grid, the advection velocities were reversed. The results of the experiment are shown in Fig. 7. The calculation worked reasonably well, but not perfectly.

Telescoping grids cause reflection problems similar to those created by boundary conditions. Some of the shorter wave components are reflected at the interface between differing mesh intervals in a telescoping grid. Figure 8 shows a 1-dimensional telescoping grid--a coarse-mesh region (CM) surrounding a refined mesh (RM) (mesh ratio = 4:1). A Gaussian which satifies the

---

* An even more effective procedure is to use the Galerkin method to derive an equation for the outflow point. This will be covered in a future report.

non-linear advection equation passes from the CM region into the RM region and back into CM. Waves are reflected at both interfaces but particularly at the RM-CM boundary. Figures 9 and 10 show the possible utility of gradually reducing the mesh ratio; the ratio is changed from 4:1 to 4:2:1. This gradual reduction in the mesh ratio resulted in an apparent reduction of the wave reflections at the RM-MRM (moderately refined mesh) interface and at the MRM-CM interfaces.

9. Summary

Chapeau functions are used in the TDL boundary layer model to integrate the horizontal portions of the predictive equations for temperature, wind, and humidity. Chapeau functions, a special case of the Galerkin method, permit the use of longer time steps than would be allowed by usual explicit techniques. For the case of constant 1-dimensional advection, chapeau functions exhibit fourth-order spatial accuracy, can be made absolutely stable and are non-dissipative.

The extension to a 2 or 3-dimensional grid can be carried out by using Marchuk's "splitting" technique.

Fixed outflow boundary values may create "ghosts" at the inflow boundary. The diffuculty may be alleviated by using an implicit upstream differencing scheme at the outflow boundary.

Telescoping grids create related problems. The interface between a refined-mesh and a coarse-mesh region seems particularly prone to reflection difficulties.

10. References

1. Shaffer, W. A., and P. E. Long, 1975: A predictive boundary layer model. NOAA Tech. Memo. TDL-57, 41 pp.

2. Long, P. E., 1975: Dissipation, dispersion and difference schemes. NOAA Tech. Memo. TDL-55, 33 pp.

3. Long, P. W., and W. A. Shaffer, 1975: Some physical and numerical aspects of boundary layer modeling. NOAA Tech. Memo. TDL-56, 37 pp.

4. Finlayson, B. A., 1972: The method of weighted residuals and variational principles. Mathematics in Science and Engineering, Vol. 87, Academic Press, New York, 412 pp.

5. Yanenko, N. A., 1971: The method of fractional steps. Heidelberg, Springer-Verlag, 160 pp.

Appendix I

List of Major Symbols

c	Phase speed
CM	Coarse Mesh Region
D_-	Difference operator with effect of $D_- Q_j = \frac{Q_j - Q_{j-1}}{\Delta x}$
D_x	Fourth-order central difference operator
e_i	Chapeau basis function
g	Amplification factor
$g(x,t)$	Forcing function in non-linear advection equation
h_j	$h_j = x_{j+1} - x_j$ for irregularly spaced grids
i	$\sqrt{-1}$
j	Finite-difference spatial index
L_x, L_y	Spatial difference operators for the x and y directions
MRM	Moderately refined mesh
n	Time step index
$\mathcal{O}(\Delta x^p)$	Order of magnitude
Q_j^n	Arbitrary scalar variable at time level n and point j
R	Ratio of $\frac{U\Delta t}{\Delta x}$ often referred to as the Courant number
RM	Refined mesh

T	Spatial averaging operator
u	Horizontal wind speed in non-linear problems
U	Horizontal wind speed for linear cases
V	Wind vector
α_i	Time-dependent chapeau function coefficient for scalar variable Q
β_j	Time-dependent chapeau function coefficient for variable advective velocity
Δx, Δt	Finite difference time and space increments
$\stackrel{\bullet}{=}$	Approximate equality
$\equiv$	Equivalent to
δ	Central difference operator
$\delta_{i,j}$	Kronecker delta; $S_{i,j} \begin{cases} 0, i \neq j \\ 1, i=j \end{cases}$
λ	Wave number
μ	Weighting factor
ϕ	Represents $\tan^{-1}(\frac{y}{x})$ where y is imaginary part and x real part of a complex variable

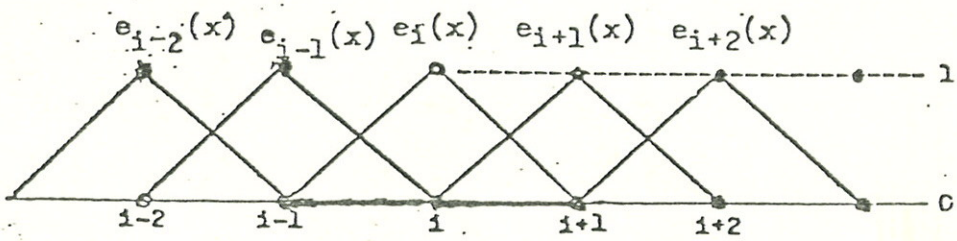

Fig. 1. The chapeau function e_i is defined as unity at the grid point i and decreases linearly to zero at grid points i-1 and i+1. Elsewhere function is zero.

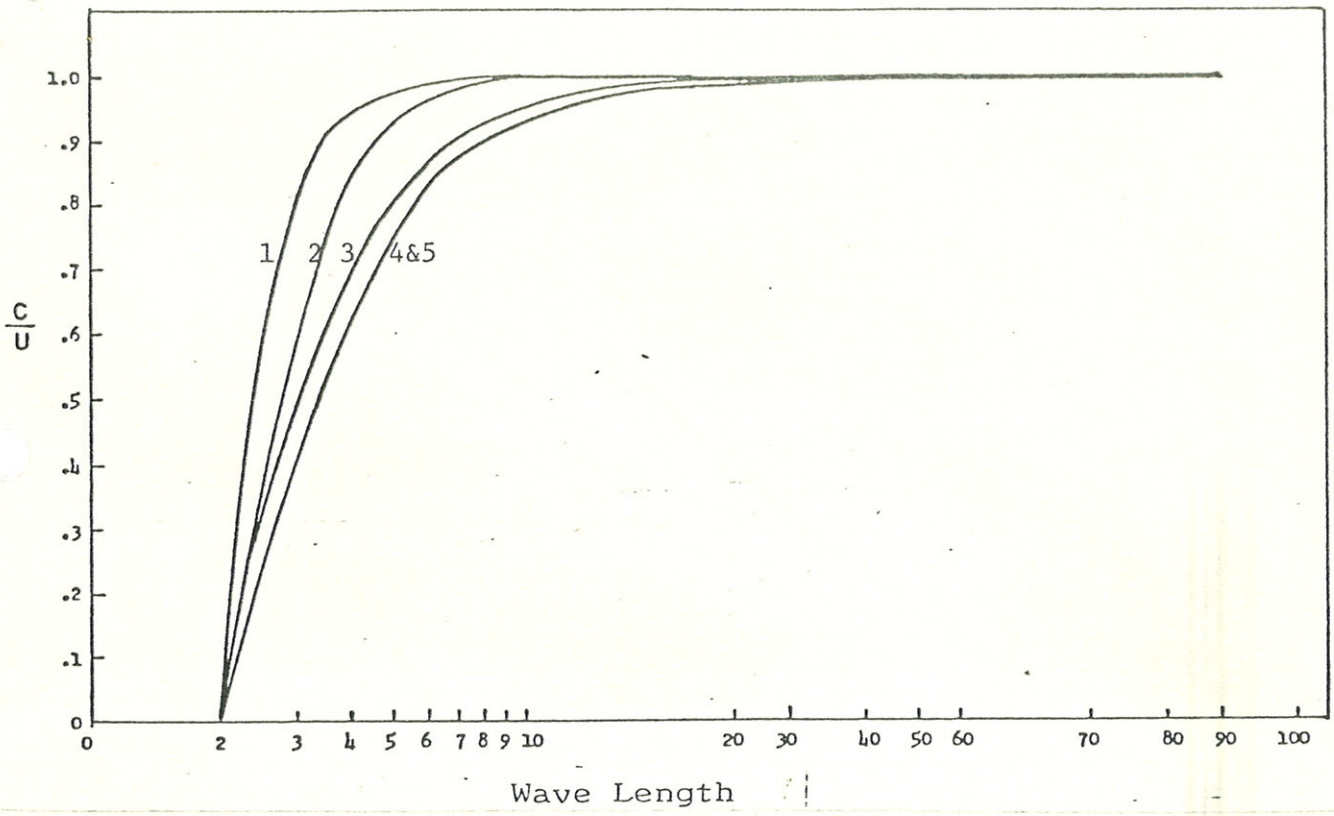

1. Chapeau Function

$$1/6\ [(Q^{n+1}_{j-1} - Q^{n}_{j-1}) + 4(Q^{n+1}_{j} - Q^{n}_{j})\ \ (Q^{n+1}_{j+1} - Q^{n}_{j+1})] + R/2\ [\mu(Q^{n+1}_{j+1} - Q^{n+1}_{j-1}) + (1-\mu)\ (Q^{n}_{j+1} - Q^{n}_{j-1})] = 0, \quad \mu = 1/2$$

2. 4th Order Crank-Nicolson

$$\frac{Q^{n+1} - Q^{n}}{\Delta t} + \frac{U}{2\Delta X}\ (Dx\ Q^{n+1}_{j} + Dx\ Q_{j}) = 0 \quad \text{where } DxQ_{j} = 2/3\ (Q_{j+1} - Q_{j-1}) - 1/2\ (Q_{j+2} - Q_{j-2})$$

3. Upstream

$$\frac{Q^{n+1} - Q^{n}}{\Delta t} + \frac{U}{\Delta X}\ [\mu(Q^{n+1}_{j} - Q^{n+1}_{j-1}) + (1-\mu)\ (Q^{n}_{j} - Q^{n}_{j-1})] = 0, \quad \mu = 0$$

4. Leap-frog

$$\frac{Q^{n+1}_{j} - Q^{n-1}_{j}}{2\Delta t} + \frac{U}{2\Delta X}\ [(Q^{n}_{j+1} - Q^{n}_{j-1})]$$

5. 2nd Order Crank-Nicolson

$$\frac{Q^{n+1}_{j} - Q^{n}_{j}}{\Delta t} + \frac{U}{2\Delta X}\ [\mu(Q^{n+1}_{j+1} - Q^{n+1}_{j-1}) + (1-\mu)\ (Q^{n}_{j+1} - Q^{n}_{j-1})] = 0, \quad \mu = 1/2$$

Fig. 2. Phase velocities as a function of wavelength for finite difference schemes listed above.

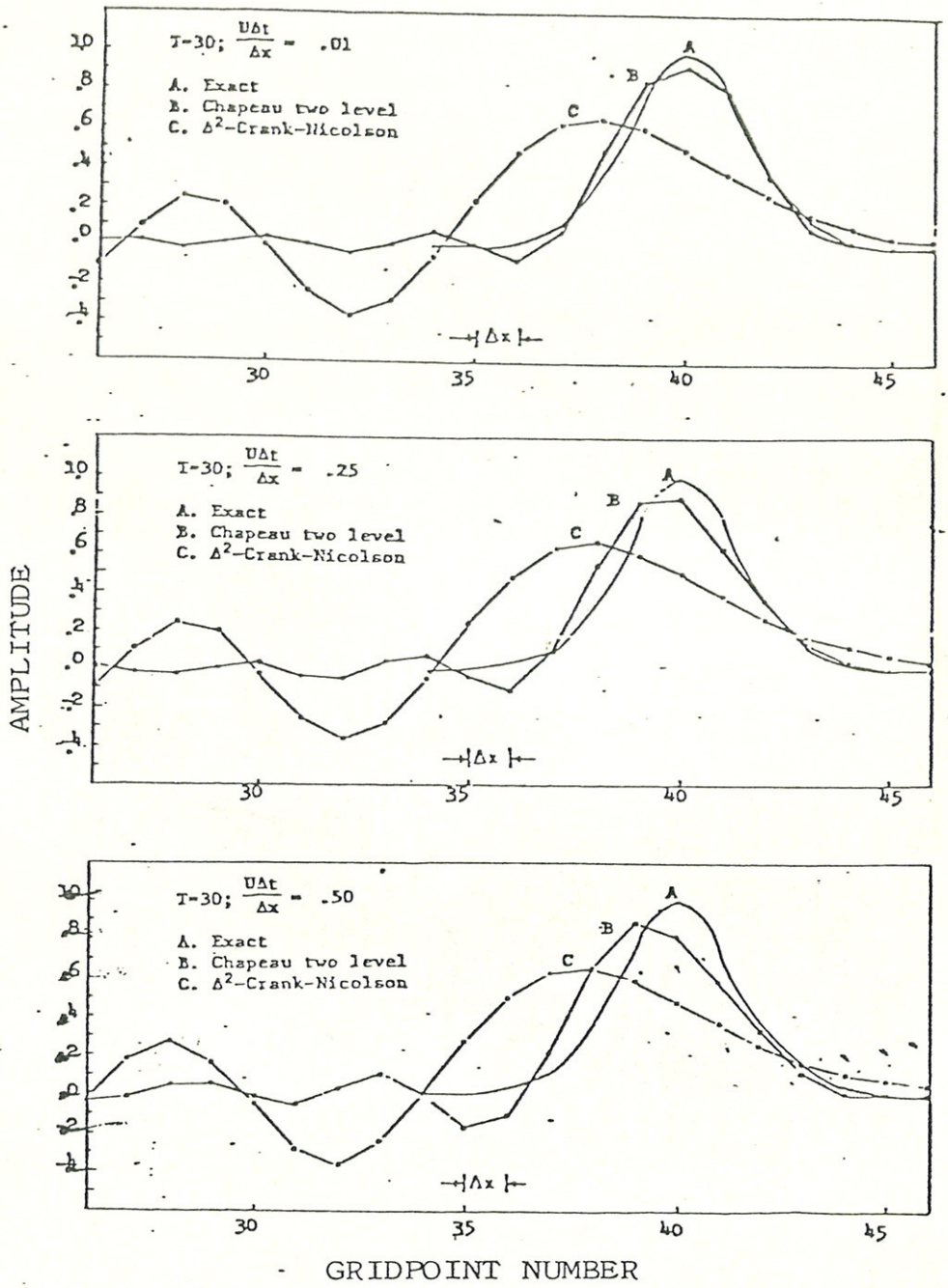

Fig. 3. Comparison of solutions of the 1-dimensional advection equations using a two-level chapeau function scheme and a second order Crank-Nicolson scheme.

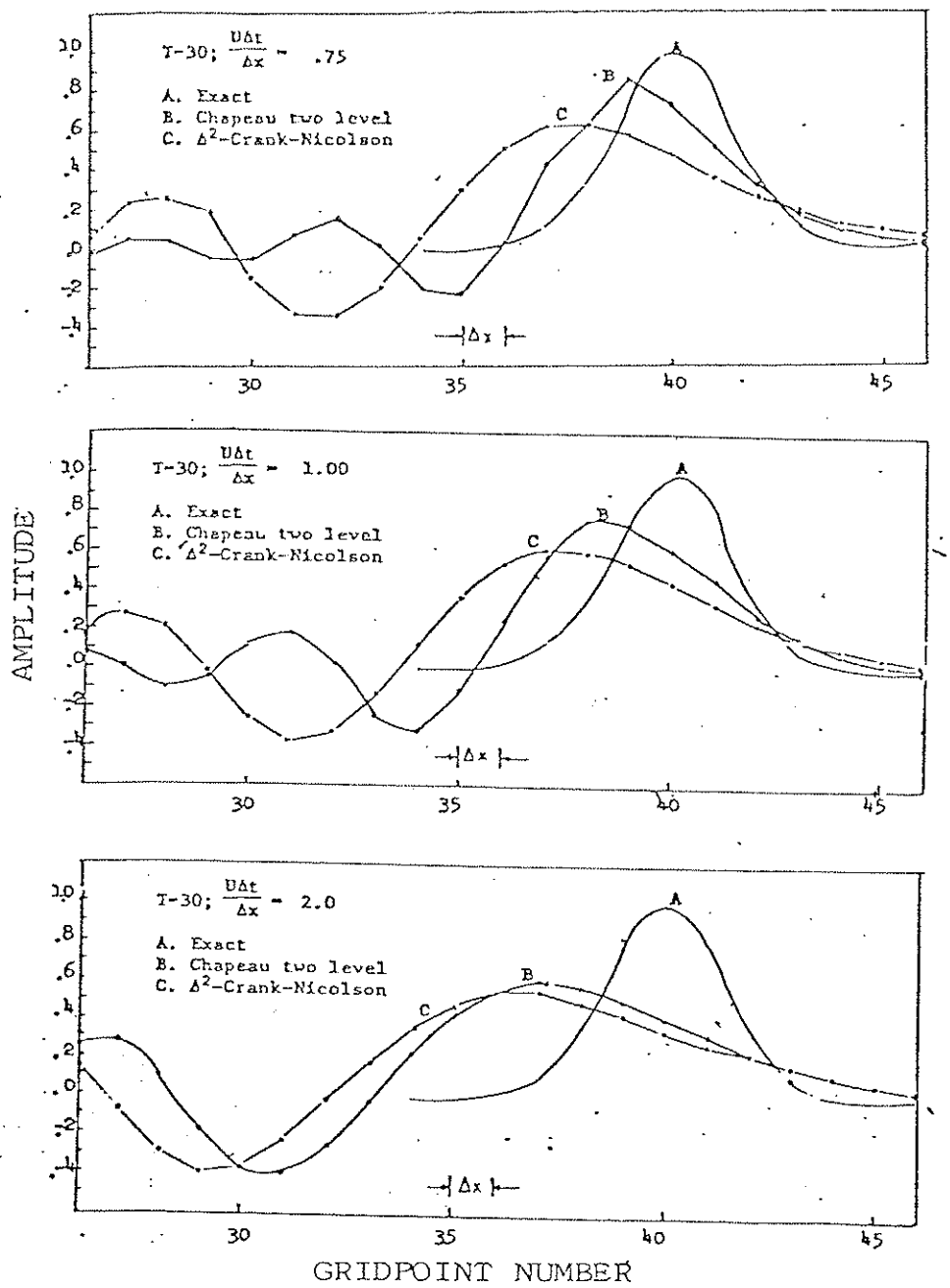

Fig. 4. Extension of Fig. 3 for larger timesteps.

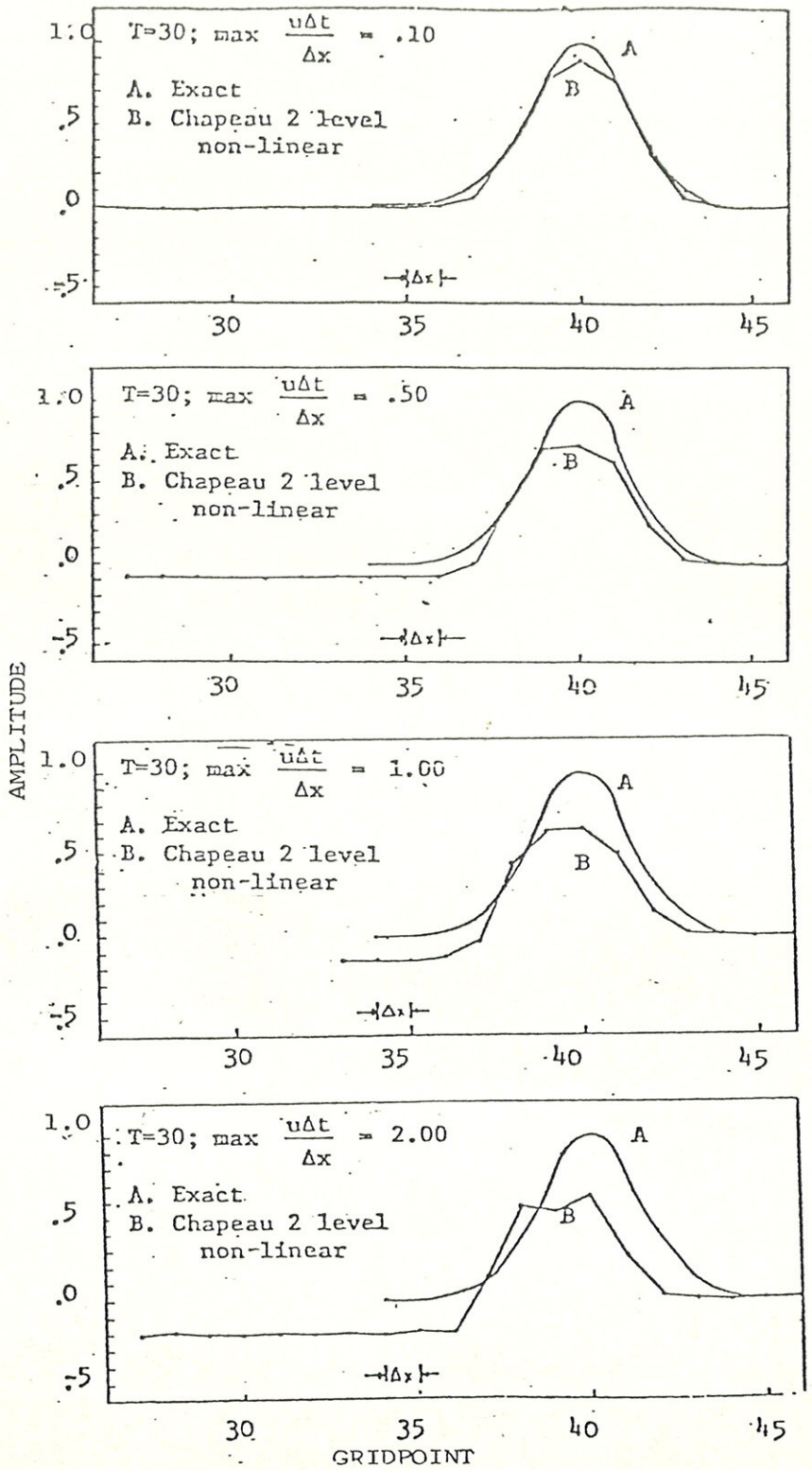

Fig. 5. A chapeau function solution for the nonlinear advection equation is compared to the exact solution. A two level chapeau function is used.

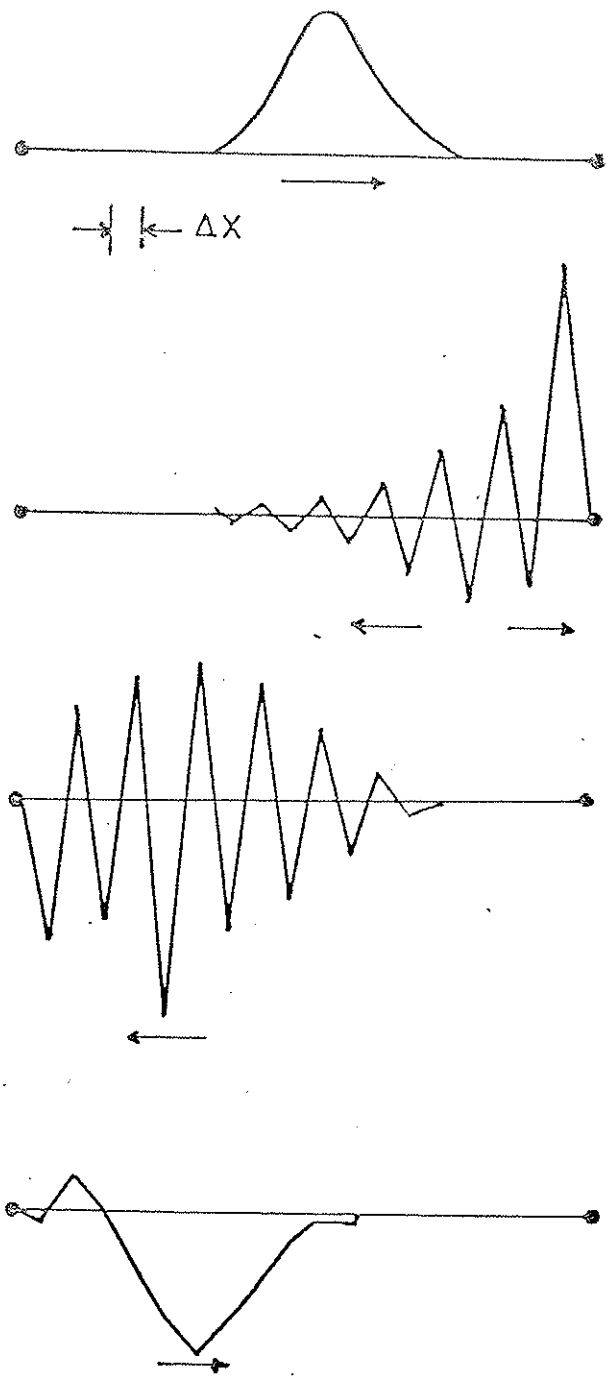

Fig. 6. Conjuration of a "ghost" using a fixed outflow boundary value.. Outflow and inflow points are denoted by (•).

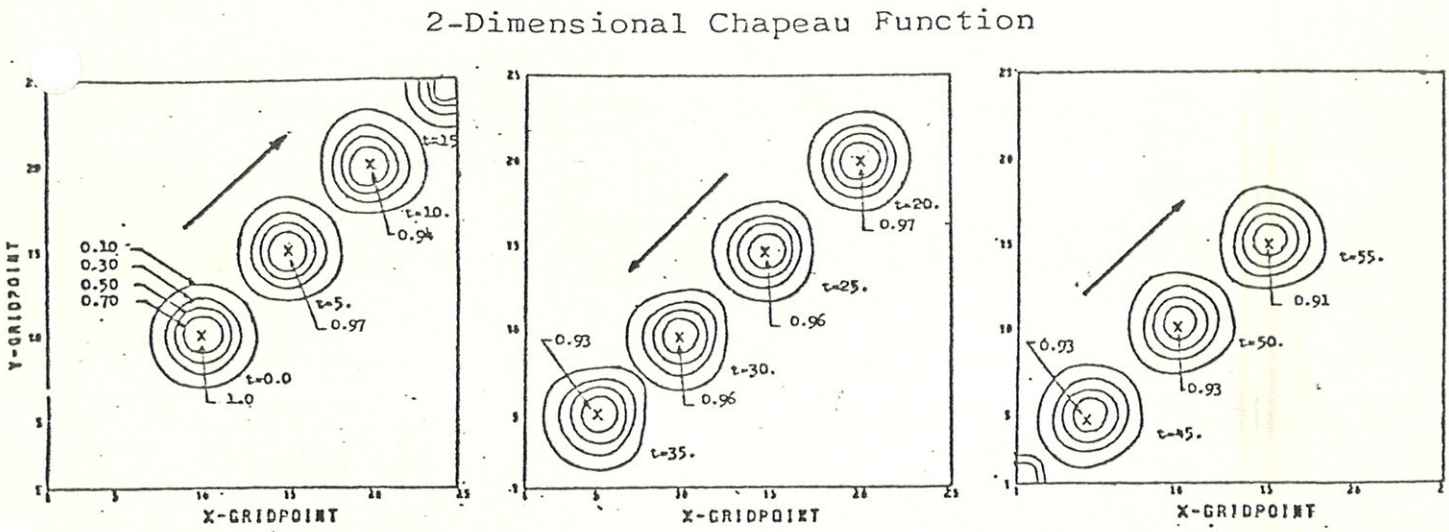

Fig. 7. A two dimensional Gaussian with an amplitude of 1 is advected by a chapeau function scheme. Marchuk's splitting technique, which allows the advection to be treated as two one-dimensional problems, is used. In this test, the advecting velocity is reversed when the exact center of the Gaussian meets a corner.

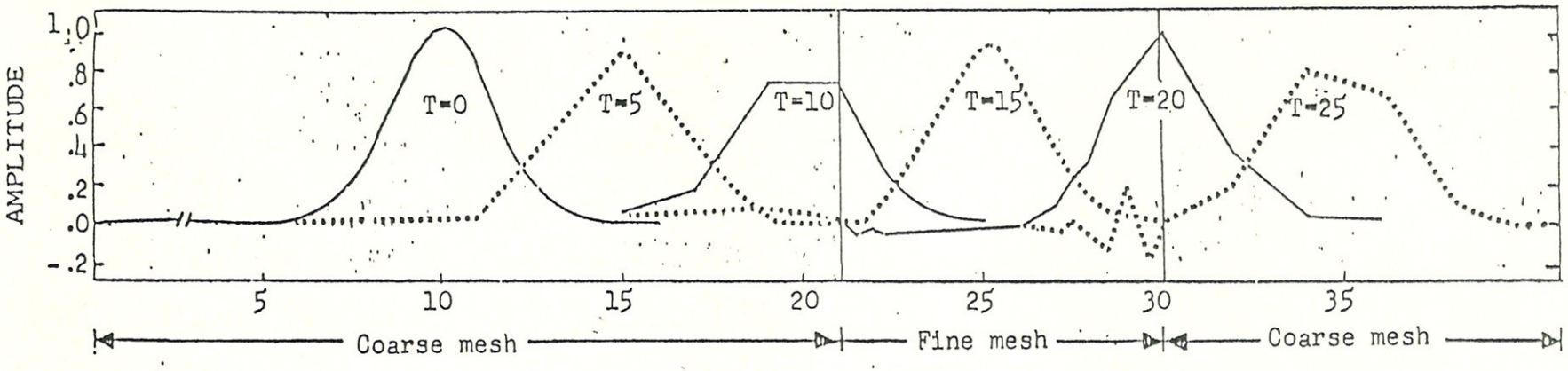

Fig. 8. Evolution of a Gaussian solution to the non-linear advection equation, $\frac{\partial Q}{\partial t} + u(x,t) \frac{\partial Q}{\partial x} = g(x,t)$. Here, once again, chapeau functions advect the Gaussian. Note that when the Gaussian passes from coarse mesh (x = 21) and back into the coarse mesh at x = 30, small amplitude waves are generated.

$\Delta t = 0.1$; $(\Delta x)_{coarse} = 2$; $(\Delta x)_{fine} = .5$; Max u = 1.

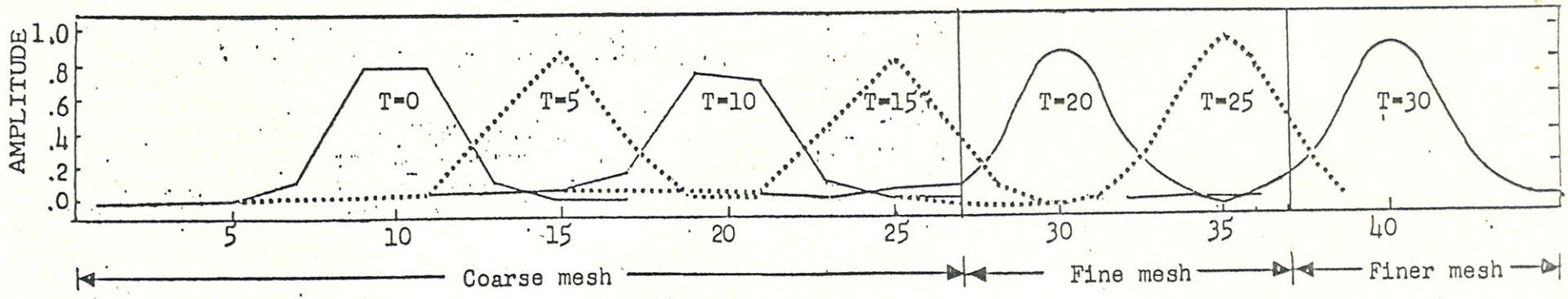

Figure 9. Evolution of a Gaussian solution to the non-linear advection equation $\frac{\partial Q}{\partial t} + u(x,t)\frac{\partial Q}{\partial t} = g(x,t)$. A Gaussian is advected from a coarse mesh (CM) region, through a medium refined mesh region (MRM) and finally into a refined mesh region (RM). Chapeau functions are used to advect the object.

$\Delta t = 0.1$; $(\Delta x)_{coarse} = 2$; $(\Delta x)_{fine} = 1.$; $(\Delta x)_{finer} = 1/2$; Max u = 1.

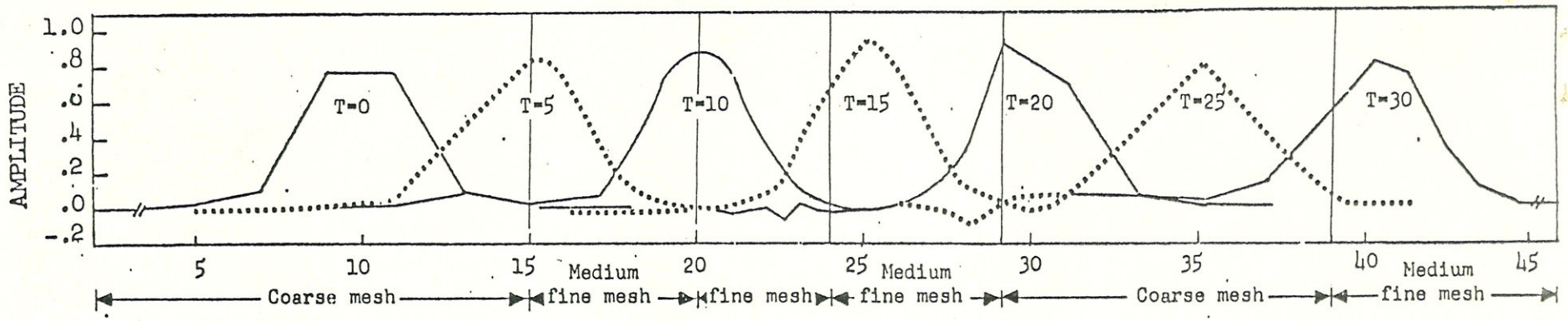

Fig. 10 Similar to figure 9. A Gaussian is advected from a CM region through a MRM region to RM region to MRM to CM to MRM region. Chapeau functions are used to advect the object.

$\Delta t = 0.1$; $(\Delta x)_{CM} = 2.$; $(\Delta x)_{MRM} = 1.$; $(\Delta x)_{RM} = 1/2$; Max $u = 1.$